A 500°C Isothermal Section for the Al-Au-Cu System

F.C. LEVEY[1], M.B. CORTIE[2], L.A. CORNISH[3]

The Al-Au-Cu system and its associated ternary alloys and intermetallic compounds is surprisingly poorly known, and the authors could find no phase diagram for it in the literature. This paper addresses this omission by presenting an isothermal section at 500°C, derived with the aid of X-ray diffraction (XRD), energy dispersive spectroscopy (EDS), metallography and hardness measurements. The samples studied had generally received an anneal of 2 hours at 500°C, primarily in order to complete any transformations that occurred during solidification and cooling of the castings. The possibility of further changes on protracted annealing at 500°C is not ruled out, and the diagram presented is therefore applicable only to material prepared by thermal processing of an industrial nature. The presence of a ternary β phase with a nominal stoichiometry of $AlAu_{2-x}Cu_{1+x}$, $0 \leq x \leq 1$ was confirmed, and its phase field at 500°C determined. A number of the binary intermetallic phases were found to exhibit some solid solubility of the ternary element. In particular, the γ Al_4Cu_9 phase extends deep into the ternary and, in the vicinity of the commercially interesting 18 carat line, appears to exist in a ternary ordered form, designated here as γ_2.

---

[1] 2600 Natta Blvd., Bellmore, NY 11710, USA, formerly Engineer with Mintek, South Africa

[2] Manager, Physical Metallurgy Division, Mintek, Private Bag X3015, Randburg 2125, South Africa

[3] Associate Professor, School of Process and Materials Engineering, University of the Witwatersrand, South Africa

I. INTRODUCTION

A family of Al-Au-Cu jewelry alloys with an unusual sparkling surface finish (‘Spangold’) was developed in the early 1990s at Mintek, in South Africa.(1-3) At that time, the metallurgy of these alloys was not understood, and no prior literature was found on the particular compositions of interest. The structure of the alloy with the stoichiometry $Al_4Au_7Cu_5$ was subsequently determined from diffraction data, and it proved to have an ordered B2 crystal structure at temperatures above about 80°C and a nominally tetragonal martensite at temperatures below 30°C. (4-6) The properties of this phase indicated that it was a ternary example of a Hume-Rothery β electron phase.(7) It is also of interest because it has shape memory properties and because it straddles the commercially relevant 18 carat (75 wt.% Au) section. Its range of stability is referred to here as the ‘ternary β phase field’.

In the present work, the extents of the β and other phases in the ternary Au-Cu-Al system have been determined, and a 500°C isothermal section has been constructed. The motivation for this work was firstly to address the omission in the literature (as, for example in references (8) or (9)), and secondly to provide information that could be used to optimize alloys for jewelry and shape memory applications. The isothermal section is not proposed as a true equilibrium phase diagram, because annealing times were in general only two hours at 500°C. Rather, the diagram presented should be seen as being applicable mainly to the cast-and-solution-anneal thermal histories typical of industrial processing. This work was performed in parallel with a determination of the 76 wt % Au vertical section. Therefore, about half of the samples studied contained 75 or 76 wt % Au.

II. EXPERIMENTAL PROCEDURES

Samples were prepared by either arc-melting or air-melting elements of at least 99.9 % purity. The compositions of the samples were analyzed by EDS in a JEOL 840 SEM at 20 kV using elemental standards. The reliability of the analyses was also confirmed by analyzing binary line compounds. All the compositions in this paper are given in atomic percent, unless otherwise indicated. In general, the samples were annealed in air at 500°C for two hours and then quenched into a mixture of ice and water, or ice and brine. Selected samples received anneals in vacuum of up to 100 hours in order to determine whether further microstructural changes were likely to occur. Each sample was polished to a 0.25 µm finish using a diamond suspension, and some were polished further to a 0.1 µm finish using a gamma alumina suspension. A combination of EDS phase composition analyses, X-ray diffraction (XRD), peak matching from spectra of known phases in the JCPDS database,(10) and metallography were used to elucidate the phases present in these samples. The structures of the phases that could not be matched with previously documented phases were determined from the XRD spectra, as described elsewhere.(4-6) Optical metallography was generally performed after etching with 0.1g CrO_3 in 10 ml HNO_3 + 100 ml HCl, which was satisfactory for alloys with gold contents above about 30 at. %. However, less noble samples were susceptible to rapid, selective removal of Al and Cu, which caused the surface to become obscured by a blanket-like layer of gold. Acid ferric chloride or aqua regia proved to be a better choice for such alloys. In addition, some of these alloys were examined in the unetched condition using Nomarski interference.

III. RESULTS

A. *Composition and Structural Analysis*

The analyzed compositions of the samples and their constituent phases are given in Table I.

The ternary β phase could usually be identified from its characteristic microstructure (Figure 1), which contained laths formed during the martensitic transformation of the parent B2/L2_1 phase (which have been previously studied in some detail by the authors (5,11,12)), its intermediate range of hardness values (extending from 180 to 360 HV), its nominally tetragonal X-ray diffraction spectrum, and its chemical analysis.

Many of the samples contained the face centered cubic (fcc) α phase, which in these alloys is a disordered solid solution of Au and Cu. Such samples had hardnesses of only 100 to 180 HV, which together with their fcc X-ray diffraction spectra made identification of the microstructure straightforward. However, as is well known, the stoichiometries 3Au:1Cu, 1Au: 1Cu and 1Au: 3Cu will form the ordered phases Au_3Cu, AuCu and $AuCu_3$ respectively below 500°C. In some cases, such ordered phases did form in the samples, and their lath-like optical microstructures appeared superficially similar to those of the β phase, while their hardness values extended as high as 290 HV. However, they could be differentiated from the β phase by a consideration of their X-ray diffraction spectra and by chemical analyses. It is possible that these ordered compounds were formed during cooling after the anneal at 500°C, since they are not present in the Au-Cu binary diagram at 500°C. The occurrence of these ordered phases will therefore be ignored in the following discussion.

The phase Al_2Au (also known as ‘purple glory’(13)) was readily identified from its vivid purple color, its narrow stoichiometry and its X-ray diffraction spectrum. The other binary compounds were identified from their stoichiometry, which (with one exception discussed below) was relatively restricted.

An unexpected discovery was the presence of a phase lying between β and Al_2Au on the 18 carat line. This phase is designated γ_2 in Table I, and will be discussed further in the following section. The γ_2 phase was brittle, with a hardness of between 550 and 860 HV, depending on composition.

The structure of some of the phases was investigated with the aid of Crystallographica[♦] , a software package that calculates X-ray diffraction spectra from user-defined unit cells. In particular, the unit cell dimensions and lattice atomic occupancy of the γ phase were varied, and the resulting structures used to calculate XRD spectra, which were then compared to the experimental spectra.

[♦] Crystallographica is a product of Oxford Cryosystems, 3 Blenheim Office Park, Lower Road, Long Hanborough, Oxford OX8 8LN, UK.

B. *Determining the Ternary Extension of the γ Phase*

It was originally anticipated by the authors that the order of the phases obtained on progressively substituting Al for Cu along the 18 carat (75 wt.% Au) section of the ternary would be fcc α- (Au,Cu), then the bcc β electron phase with the nominal formula $AlAu_2Cu$, and finally the purple intermetallic compound Al_2Au (which has the CaF_2 structure). Metallographic examination of the samples proved, however, that there was a fourth phase, intermediate in composition between the Al_2Au and the β. At first we confused this phase with β, as in references (4), (7) and (12). This confusion was abetted by initial analyses of the new phase's XRD spectrum, which indicated that it was nominally bcc, with lattice parameters of 0.306 nm (or multiples thereof). This is very nearly the same as that of the β phase, which was found to have a lattice parameter of 0.308 nm when indexed as B2 body centered cubic.(4) However, examination of a comprehensive set of metallographic specimens showed the presence of fine duplex microstructures consisting of light pink dendrites of the new phase, and either yellow β (Figure 2) or purple Al_2Au (Figure 3), depending on the overall composition of the sample, proving that a separate phase was present.

The composition of the new phase suggested that it might be an extension of either $AlAu_2$ (since it had a stoichiometry that could be written as $Al(Au,Cu)_{2.2}$) or of the γ-electron phase Al_4Cu_9, with a stoichiometry of $Al_4(Cu_{0.4}Au_{0.6})_9$. However, an analysis of the relevant XRD spectra revealed that its crystal structure was closely related to that of the γ electron phase (Figure 4). It is interesting to note that the γ structure is often described as a complex bcc structure with certain atoms removed,(14) which explains our initial error. The lattice parameter of the new phase was, however, relatively larger than that of the standard Al_4Cu_9. This could be explained by noting that the atomic radius of Au is nominally 0.144 nm while that of Cu is only 0.128 nm. Substituting Au for Cu in the ratios 4:6, and assuming that the very simple linear law of Vegard applies, should have caused the unit cell parameters to expand to ~0.899 nm for $Al_4(Cu_{0.6}Au_{0.4})_9$. When the ratio of Au to Cu was 6:4, as in $Al_4(Cu_{0.4}Au_{0.6})_9$, the predicted unit cell parameter would be ~0.914 nm. In fact, the measured values from the spectra were 0.9077±0.0005 nm and 0.9175±0.0005 nm respectively, which we consider to be a satisfactory agreement given the known shortcomings of Vegard's law.(14) Interestingly, the latter of the new lattice parameters is exactly a factor of three larger than the lattice parameter determined for the initially-supposed B2 structure.

Despite the good match in the peak positions, the intensity of the peaks of the measured spectrum differed from those of the standard binary spectrum for Al_4Cu_9 (compare the calculated spectrum in Figure 5a to the measured spectra in Figures 5b and 5c). The actual peak heights could be explained by assuming that Au did not substitute randomly for Cu, and that there was actually a degree of ternary ordering involving the atoms these two elements. The resulting calculated spectrum is shown in Figure 5d, and is a reasonable representation of the measured ones. Therefore, this phase will be referred to as the γ_2 phase in the present work, since its structure appears to be produced from that of the γ phase by additional ternary ordering.

C. *Construction of the 500°C Isothermal Section*

The proposed isothermal section has been plotted in Figure 6 according to the EDS phase composition analyses of the samples annealed at 500°C, together with the structural analyses. Two versions are presented. In the first (Figure 6a) the data points and experimental tie lines are shown superposed on the derived phase boundaries, while in the second (Figure 6b) only the inferred phase boundaries and their associated three-phase and two-phase fields are given.

The α phase region extends, as expected, down the Au-Cu side of the ternary section from the α phase of (Al,Au) to the α phase of (Al,Cu). Note that at lower temperatures this phase is known to form ordered compounds of the types Au_3Cu, AuCu and $AuCu_3$, which are not shown on the 500°C section. The restriction in the α phase field adjacent to that of the ternary β phase appears to be the result of a peritectic $\alpha + L \rightarrow \beta$ transformation that occurs at elevated temperatures, and which, on solidification, converts α dendrites containing more than about 10 at.% Al to β phase.

It appears that the β phase of the nominal $AlAu_2Cu$ composition occurs as an island in between the extensions of the binary Au_4Al and $AlCu_4$ β phases into the ternary. This situation differs from one of the original possibilities considered, in which the β phase was envisaged to be part of a continuous β phase field linking the β phase fields of $AlCu_4$ and $AlAu_4$.(6) This has been observed in other systems, for example Ag-Al-Au, where the $AlAu_4$ β intermetallic compound reportedly stretches across nearly the entire ternary section at 500°C.(8)

The other interesting feature of this phase diagram is the great extent of the Al_4Cu_9 γ phase. This phase field, like many of the others, is strongly aligned along a line of constant electron-to-atom ratio, providing a fine illustration of the Hume-Rothery rules.

Also included on this section is a proposed three phase field determined from the constituent phases in the as-cast PB15 60.6 % sample, the composition of which lay within the Al_2Au-AlCu-Al_2Cu tie triangle. The microstructure (Figure 7) and the presence of this tie triangle suggests that there is at least one ternary invariant reaction, involving the liquid phase and two of the three intermetallic phases. The microstructure indicates the cooling sequence:

$L \rightarrow Al_2Au$

$L + Al_2Au \rightarrow AlCu$

$L + AlCu \rightarrow Al_2Cu$.

Dendrites of AlCu were also observed. Evidently, they are they result of directional solidification of the AlCu phase after its peritectic formation from $AuAl_2$.

IV. DISCUSSION

A. *The β Phases*

The $AlAu_4$ β phase and the ternary Al-Au-Cu β phase have a range of stoichiometry that is aligned in the direction of a constant electron-to atom ratio of about 1.5. It is probable that the $AlCu_3$ β phase also exhibits an appreciable solubility of the ternary element (Au in this case) along this line, although of course this will not visible on the 500°C section on account of $AlCu_3$ not being stable below 567°C. Therefore, given the well-known tendency of β phase fields to shrink in extent with *decrease* in temperature,(14) it is possible that the three β regions of $AlAu_4$, ternary β phase and $AlCu_4$ are contiguous at some temperature *above* 500°C, and the division arises from miscibility gaps rather than from a reaction. If so, then the present ternary β phase may not strictly speaking be a new phase, insofar as it might also be the ternary extension of one or both of the binary β phases. However, it is clearly stable at lower temperatures than either of the two binary phases, which accentuates its presence on the 500°C section.

At 500°C at least, the stability range of the ternary β phase can be approximately described as lying within a triangle with the stoichiometries $Al_{1.08}Au_{1.96}Cu_{0.96}$, $Al_{0.68}Au_{2.12}Cu_{0.80}$ and $Al_{1.0}Au_{1.0}Cu_{2.0}$ at the vertices, and with the widest range of stability centered on the stoichiometry $AlAu_2Cu$ and the narrowest on $AlAuCu_2$. It seems acceptable to describe it as having the nominal stoichiometry $AlAu_{2-x}Cu_{1+x}$, $0 \leq x \leq 1$. The triangular shape results geometrically from the fact that the locus of temperatures for the eutectoid decomposition of β appears to pass through the 500°C plane of the ternary at close to the $AlAuCu_2$ stoichiometry.

The present study has confirmed that 18 carat Spangold jewelry alloys with between 4 and 6 wt. % Al lie within the phase field of a β phase. Therefore these alloys may be expected to exhibit behavioral affinities with other shape memory alloy systems that have a parent crystal structure based on a β phase. These other β shape memory parent phases are invariably ordered as B2, $L2_1$ or DO_3, or as B2-$L2_1$ or B2-DO_3 hybrids, a complexity that applies also to $Al_4Au_7Cu_5$ - the best studied of the $AlAu_{2-x}Cu_{1+x}$ alloys.(4,11) Furthermore, thermal cycling through the martensite transformation temperature of $Al_4Au_7Cu_5$ is accompanied by lath formation and acoustic emission,(12) and the M_s and A_s temperatures of the $AlAu_{2-x}Cu_{1+x}$ alloys vary according to composition, as in other shape memory systems. The lath morphology of $AlAu_{2-x}Cu_{1+x}$ is quite similar to that of $AlCu_3$ and the other copper shape memory alloys,(15) but is substantially different from that of the low temperature β´ form of the Au_4Al phase, which is also apparently formed by a displacive phase transformation.(16) On the other hand, the crystal structure of the low-temperature form of $Al_4Au_7Cu_5$ is significantly different from those of the martensites of the copper-based shape memory alloys. (4-6) In particular, the martensite has a nominally tetragonal structure with $c/a<1$. This is a rare situation, known mainly for certain martensites of Ni-Mn-Ga and La-Ag-In. (17,18)

Curiously, the presence of a β phase in the part of the phase diagram in the vicinity of $AlAu_2Cu$ has been alluded to previously by other workers, but apparently never specifically investigated by them. Raub and Walter, for example, reported the existence of two phases in an alloy containing 8.2 % Al, 45.9 % Cu and 45.9 % Au that had been annealed at 400°C. (19) The XRD peaks of the one phase corresponded to the AuCu disordered fcc phase. The lines of the second phase corresponded to those of the 'Au_3Al' phase, but the authors thought this was unlikely. Although a composition of Au_3Al would be required for a Hume Rothery β electron phase with an *e*/*a* of 1.5,(20) the equilibrium binary AuAl β phase actually occurs at a composition of around $Au_{4.2}Al$.(16) It is thus likely that the second phase detected by Raub and Walter was $AlAu_{2-x}Cu_{1+x}$. Not surprisingly, the overall composition of their alloy falls in the proposed α + β phase region in Figure 6.

In other work, Isobe claimed that the brittle Au_4Al phase was present in an alloy with a composition of 13.3 % Al - 41.3 % Cu - 45.4 % Au. (21) This alloy exhibited the shape memory effect, which is possibly due to the same reversible transformation that occurs in the β phase of the $Al_4Au_7Cu_5$ composition. However, the composition of their alloy lies at the α edge of the α+β phase field, and contains less Au than the 18 carat $Al_4Au_7Cu_5$ alloy. It thus seems unlikely that the Au_4Al phase would be found in these alloys under equilibrium conditions, according to the proposed ternary section, and once again the phase observed appears to have been $AlAu_{2-x}Cu_{1+x}$.

However, it is interesting that when Sato and Toth (22) added up to 23 % Al to AuCu thin films, no observation of a β phase was recorded. The 23 % Al alloy investigated by these authors contained 38.5 % Cu and 38.5 % Au. If the composition of this alloy is plotted on the isothermal section of Figure 6, it falls within the proposed β phase field. This may possibly be explained by the fact that, over some compositions at least, the $AlAu_{2-x}Cu_{1+x}$ phase appears to form during solidification from the α by a peritectic transformation.(6) The $AlAu_{2-x}Cu_{1+x}$. phase boundaries above 500°C are therefore expected to be rather different to those shown in

Figure 6. In particular, the solidus surface of the α phase is expected to overlie some of the ternary β phase field. This difference might also apply to thin films, if they are in a metastable condition.

B. *Technological Implications*

Now that it has been confirmed that the 18 carat Al-Au-Cu jewelry alloys lie in a previously undocumented ternary β phase field, and the extent of this phase field and some of its associated phase transformations have been determined, it may be possible to determine the most suitable composition for jewelry or shape memory alloy manufacture. In particular, the knowledge can be used to ensure that single-phase samples are produced, free of other, possibly deleterious, intermetallic phases. This may improve the mechanical integrity of the alloy, which would, in turn, improve the commercial prospects for both jewelry and shape memory applications, since the major disadvantage of the alloy to date has been its brittle behavior.

V. CONCLUSIONS

1. The maximum solubility of Al in the (Au,Cu) α phase at 500°C varies from about 15 at.% Al at the Au-Al and Cu-Al extremities to about 10 at.% Al at 50 at.% Au. The constriction in the phase field at the 50 at.% Au level appears to be the consequence of a peritectic $L+\alpha\rightarrow\beta$ reaction.
2. A previously undocumented ternary phase, with the nominal stoichiometry $AlAu_{2-x}Cu_{1+x}$ ($0\leq x\leq 1$), is present on the 500°C section. However, it has not been determined whether this phase is contiguous at higher temperatures with Au_4Al and/or $AuCu_3$, the binary β phases in this system.
3. The $AlAu_{2-x}Cu_{1+x}$ phase field is widest around the $AlAu_2Cu$ stoichiometry. This region of the phase diagram also contains the Spangold jewelry and shape memory alloy, which has a nominal stoichiometry of $Al_4Au_7Cu_5$.
4. The Au_2Al and Au_4Al phases may contain up to about 10 and 15 at.% Cu respectively, with the Cu substituting for Au in their compositions.
5. The Al_4Cu_9 γ phase extends deep into the ternary section at 500°C, and may contain up to about 50 at.% Au, which substitutes for Cu.
6. The X-ray diffraction spectra of the Au-rich examples of the γ phase indicate that some ternary ordering of Au and Cu occurs. The new, ternary-ordered phase is designated γ_2. The nature of the phase boundary between γ and γ_2 was not determined.

Acknowledgements

This paper is published by permission of Mintek. The authors are grateful to T Biggs, S Taylor, I Klingbiel and P Ellis for undertaking the XRD and EDS measurements.

REFERENCES

1. I. M. Wolff and M.B. Cortie: *Gold Bull.*, 1994, vol. 27, no. 2, pp. 44-54.
2. I.M. Wolff and V.R. Pretorius: *Gold Technol.*, 1994, vol. 12, pp. 7-11.
3. M. Cortie, I. Wolff, F. Levey, S. Taylor, R. Watt, R. Pretorius, T. Biggs and J. Hurly: *Gold Technol*., 1994, vol. 14, pp. 30-36.
4. M.B. Cortie and F.C. Levey: *Intermetallics,* 2000, vol. 8, no. 7, pp. 793-804.
5. F.C. Levey and M.B. Cortie: *Mater. Sci. Eng.*, 2001, vol.A303, pp.1-10
6. F.C. Levey: Phase Relationships, Transformation Behaviour and Material Properties in Au-Cu-Al, PhD thesis, University of the Witwatersrand, Johannesburg, South Africa, June 2000.
7. F.C. Levey, M.B. Cortie, T. Biggs and P. Ellis: *Proc. Microsc. Soc. S. Afr.*, 1998, vol. 28, p. 18.
8. A. Prince, G.V. Raynor and D.S. Evans: *Phase Diagrams of Ternary Gold Alloys*, The Institute of Metals, London, 1990.
9. P. Villars, A. Prince and H. Okamoto : *Handbook of Ternary Alloy Phase Diagrams*, ASM International, Materials Park, Ohio, 1995.
10. *JCPDS*, version 2.16, International Center for Diffraction Data, Newtown Square, PA 19073, USA, 1995.
11. F.C. Levey and M.B. Cortie, *Proceedings of the International Conference on Solid-Solid Phase Transformations ’99,* M. Koiwa, K. Otsuka and T. Miyazaki (eds.), The Japan Institute of Metals, 1999, pp.1116-1119.

12. F.C. Levey, M.B. Cortie and L.A. Cornish: *Metall. Mater. Trans. A*, 2000, vol. 31A, pp. 1917-1923.
13. R.W. Cahn : *Nature*, 10th December 1998, vol. 396, pp.523-524.
14. C.S. Barrett and T.B. Massalski : *Structure of Metals*, McGraw-Hill, New York, 1966.
15. H. Warlimont, L. Delaey, *Progr. in Mater. Sci.*, 1974, vol. 18, pp.1-157.
16. F.C. Levey, M.B. Cortie and L.A. Cornish : *Gold Bull.*, 1998, vol. 31(3), pp.75-82.
17. A. Saxena, G.R. Barsch and D.M. Hatch: *Phase Transitions*, 1994, vol. 46, pp. 89-142.
18. V.V. Martynov: *J. de Physique IV*, Colloque, 1995, vol. 5, no. C8, pp. 91-99.
19. E. Raub and P. Walter: *Z. Metall.*, 1950, vol. 41, pp. 240-243.
20. K. Girgis: *Physical Metallurgy*, ed. R.W. Cahn and P. Haasen, 3rd ed., vol. 1, Elsevier Science, The Netherlands, 1983, pp. 219-267.
21. Y. Isobe: *Jap. Pat.*, JP 2267237, 1991.
22. H. Sato and R.S. Toth: *Phys. Rev.*, 1961, vol. 124, no.6, pp. 1833-1847.

TABLES

Table 1. Sample analyses and constitution in atomic per cent. The balance in all cases is Au.

(Note *n.d.* = not detected, *n.a.* = detected but not analyzed)

Specimen	Phases	Overall, %		Phase 1, %		Phase 2, %		Phase 3, %	
		Al	Cu	Al	Cu	Al	Cu	Al	Cu
PHD1	α	8.1	25.4	8.1	25.4	*n.d.*	*n.d.*	*n.d.*	*n.d.*
PHD2	$Au_4Al+\beta$	21.1	16.5	23.0	24.7	22.9	12.2	*n.d.*	*n.d.*
PHD3	γ	29.2	39.9	29.2	39.9	*n.d.*	*n.d.*	*n.d.*	*n.d.*
PHD4	α	9.3	55.2	9.3	55.2	*n.d.*	*n.d.*	*n.d.*	*n.d.*
PHD5	β	24.1	37.4	24.1	37.4	*n.d.*	*n.d.*	*n.d.*	*n.d.*
PHD6	β+α	25.0	49.3	25.4	48.5	21.5	54.9	*n.d.*	*n.d.*
ISO1(1)	α+duplex structure	10.7	33.5	16.1	19.7	*n.a*	*n.a.*	*n.a.*	*n.a.*
ISO2	$Au_2Al+\gamma$	32.3	14.0	32.3	19.7	33.2	11.4	*n.d.*	*n.d.*
ISO3	β+α	15.5	28.7	16.6	29.2	13.6	28.5	*n.d.*	*n.d.*
ISO4	β+α	15.1	42.3	17.6	35.7	14.3	45.0	*n.d.*	*n.d.*
ISO5	$AuAl+Au_2Al+\gamma$	42.0	9.3	48.8	2.0	33.9	11.2	34.0	19.1
ISO6	β+γ	29.5	24.1	31.4	23.4	27.7	24.1	*n.d.*	*n.d.*
ISO7	β+γ	28.4	29.9	30.9	29.0	25.8	28.7	*n.d.*	*n.d.*
ISO8	α	10.7	33.5	10.7	33.5	*n.d.*	*n.d.*	*n.d.*	*n.d.*
ISO9	β	23.4	38.0	24.8	39.0	*n.d.*	*n.d.*	*n.d.*	*n.d.*
ISO10	γ	33.0	32.2	33.0	32.2	*n.d.*	*n.d.*	*n.d.*	*n.d.*
PB0	α	0.0	46.8	0.0	46.8	*n.d.*	*n.d.*	*n.d.*	*n.d.*
PB1.5	α	7.0	42.8	7.0	42.8	*n.d.*	*n.d.*	*n.d.*	*n.d.*
PB3	α	11.5	38.3	11.5	38.3	*n.d.*	*n.d.*	*n.d.*	*n.d.*
PB3A(2)	α	*n.a*	*n.a*	11.2	38.3	*n.d.*	*n.d.*	*n.d.*	*n.d.*
PB4	α+β	16.5	37.1	12.6	46.6	17.6	35.2	*n.d.*	*n.d.*
PB5	β	19.2	34.1	19.2	34.1	*n.d.*	*n.d.*	*n.d.*	*n.d.*
PB7(3)	β+γ	26.9	29.9	31.8	26.0	*n.a.*	*n.a.*	*n.d.*	*n.d.*
PB75	β+γ	28.5	28.4	30.6	28.0	25.3	27.6	*n.d.*	*n.d.*
PB8	γ	30.9	27.9	30.9	27.9	*n.d.*	*n.d.*	*n.d.*	*n.d.*
PB9	$AuAl_2+\gamma$	33.6	25.4	61.4	3.4	31.8	26.1	*n.d.*	*n.d.*

PB10	$AuAl_2+\gamma$	38.6	21.3	65.4	1.6	33.1	25.8	*n.d.*	*n.d.*
PB15(4)	$AuAl_2+CuAl_2+CuAl$	60.9	24.1	62.3	5.8	66.1	33.7	48.1	51.5
PB20	$AuAl_2+\gamma$	62.2	3.5	65.4	1.2	32.3	22.7	*n.d.*	*n.d.*
PB24	$AuAl_2+Al$	68.4	0.4	99.6	0.1	66.3	0.4	*n.d.*	*n.d.*
Al0	α	0.0	49.0	0.0	49.0	*n.d.*	*n.d.*	*n.d.*	*n.d.*
Al0.5	α	0.0	43.5	0.0	43.5	*n.d.*	*n.d.*	*n.d.*	*n.d.*
Al1	α	2.9	46.6	2.9	46.6	*n.d.*	*n.d.*	*n.d.*	*n.d.*
Al1.5	α	6.0	44.6	6.0	44.6	*n.d.*	*n.d.*	*n.d.*	*n.d.*
Al2(5)	α	8.2	42.4	2.6	47.9	*n.d.*	*n.d.*	*n.d.*	*n.d.*
Al3(6)	α+β	12.9	40.2	7.5	48.8	11.1	38.4	*n.a.*	*n.a.*
Al3.5	α+β	13.6	38.6	11.4	43.7	14.8	36.8	*n.d.*	*n.d.*
Al4.5	β	19.2	34.5	19.2	34.5	*n.d.*	*n.d.*	*n.d.*	*n.d.*
Al5	β	14.4	36.7	14.4	36.7	*n.d.*	*n.d.*	*n.d.*	*n.d.*
Al6	β	23.9	31.8	23.9	31.8	*n.d.*	*n.d.*	*n.d.*	*n.d.*
Al75	β+γ	29.3	28.1	30.6	28.4	25.3	27.9	*n.d.*	*n.d.*
ISO11(3)	$Au_4Al+\beta$	20.8	21.2	21.1	15.2	*n.a.*	*n.a.*	*n.d.*	*n.d.*
ISO12	β+γ	*n.a.*	*n.a.*	28.8	40.5	25.9	42.5	*n.d.*	*n.d.*
ISO14	α+β	18.5	46.4	22.3	36.7	17.8	48.2	*n.d.*	*n.d.*
ISO15	$AuAl_2+\gamma$	*n.a.*	*n.a.*	61.2	7.2	34.6	51.8	*n.d.*	*n.d.*
ISO16	$AuAl_2+\gamma$	54.1	16.3	64.7	4.0	34.8	36.8	*n.d.*	*n.d.*
ISO19	γ+α	20.7	57.1	30.5	46.1	21.4	56.4	*n.d.*	*n.d.*
ISO20	γ	33.0	56.9	33.0	56.9	*n.d.*	*n.d.*	*n.d.*	*n.d.*
ISO21	γ+α	30.3	56.3	31.0	55.4	24.7	62.6	*n.d.*	*n.d.*

Notes

(1) The duplex structure was too fine to analyze accurately in the SEM, but appeared to comprise a fine-scale mixture of β and Au_4Al.

(2) This sample was noticeably cored. The composition given is that of the ‘matrix’.

(3) The β phase was too fine too to analyze accurately in the SEM.

(4) This sample was analyzed in the as-cast condition. Since the analyzed intermetallic phases are stable up to their melting points in the case of $AuAl_2$ and to at least 600°C in the case of the CuAl and $CuAl_2$, it has been assumed that these structures are also present at 500°C in the ternary alloys.

(5) This sample was noticeably cored. The composition given is that of the dendrite.

(6) This sample was noticeably cored. The compositions given are that of dendrite core and matrix, in that order.

FIGURE CAPTIONS

Fig. 1- Martensitic microstructure of $Al_4Au_7Cu_5$ phase, showing laths produced by the $\beta \rightarrow$martensite displacive transformation.

Fig. 2- Duplex microstructure consisting of $Al_4Au_7Cu_5$ β phase and γ_2, in the 27.9 % Al - 29.5 % Cu sample, with a nominal composition of 76 wt.% Au - 7 wt.% Al.

Fig. 3- Duplex microstructure consisting of γ_2 and Al_2Au, in the 52.7 % Al - 9.8 % Cu sample, with a nominal composition of 76 wt.% Au – 15 wt.% Al.

Fig. 4- Spectrum of phase γ-Al_4Cu_9 , as recorded in JC-PDF database as Card 24-3.

Fig. 5- Comparison of calculated and measured spectra for new ternary phase. a. Calculated for Al_4Cu_9 assuming expanded lattice and no ternary ordering of Au and Cu; b. measured for $Al_4(Au_{0.4}Cu_{0.6})_9$; c. measured for $Al_4(Au_{0.6}Cu_{0.4})_9$; d. calculated for $Al_4(Au_{0.6}Cu_{0.4})_9$ assuming ternary ordering.

Fig. 6- 500°C section of ternary phase diagram for Al-Au-Cu system. a. data points, tie-lines and postulated phase boundaries; b. postulated phase boundaries and their associated two- and three-phase regions. The position of the 18 carat (75 wt.% Au) line is also shown.

Fig. 7- Microstructure of sample whose overall composition lay within the tie-triangle of Al_2Au-Al_2Cu and AlCu, showing a non-equilibrium microstructure produced by the peritectic consumption of Al_2Au and AlCu to produce Al_2Cu.

FIGURES

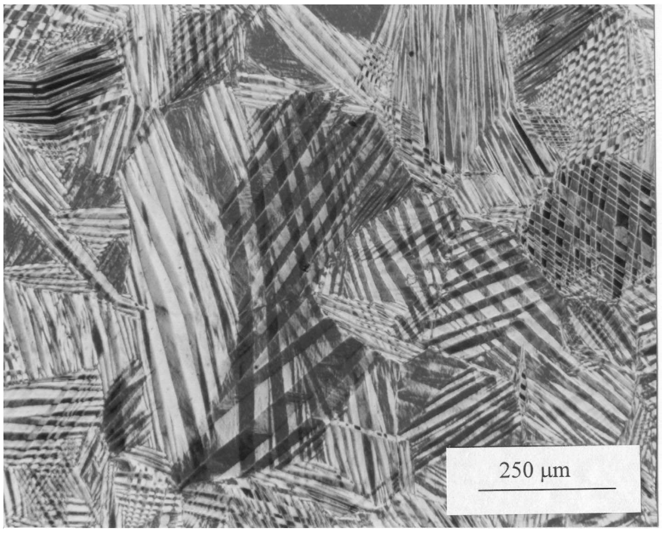

Figure 1. Martensitic microstructure of $Al_4Au_7Cu_5$ phase, showing laths produced by the $\beta \rightarrow$martensite displacive transformation.

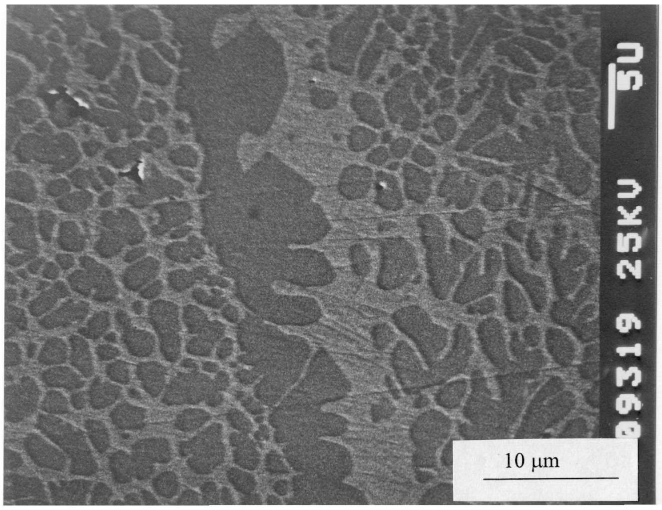

Fig. 2- Duplex microstructure consisting of $Al_4Au_7Cu_5$ β phase and γ_2, in the 27.9 % Al - 29.5 % Cu sample, with a nominal composition of 76 wt.% Au - 7 wt.% Al.

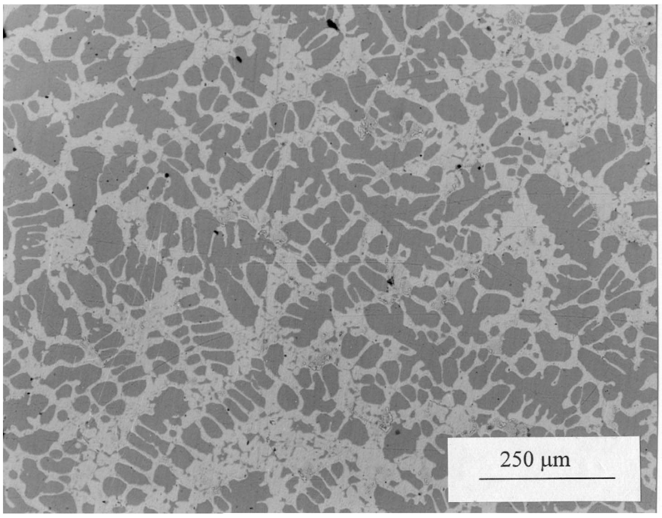

Fig. 3- Duplex microstructure consisting of γ_2 and Al_2Au, in the 52.7 % Al - 9.8 % Cu sample, with a nominal composition of 76 wt.% Au – 15 wt.% Al.

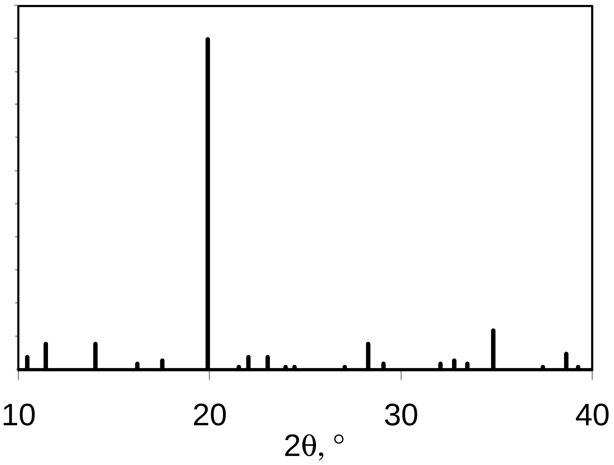

Figure 4. Spectrum of phase γ-Al_4Cu_9 , as recorded in JC-PDF database as Card 24-3.

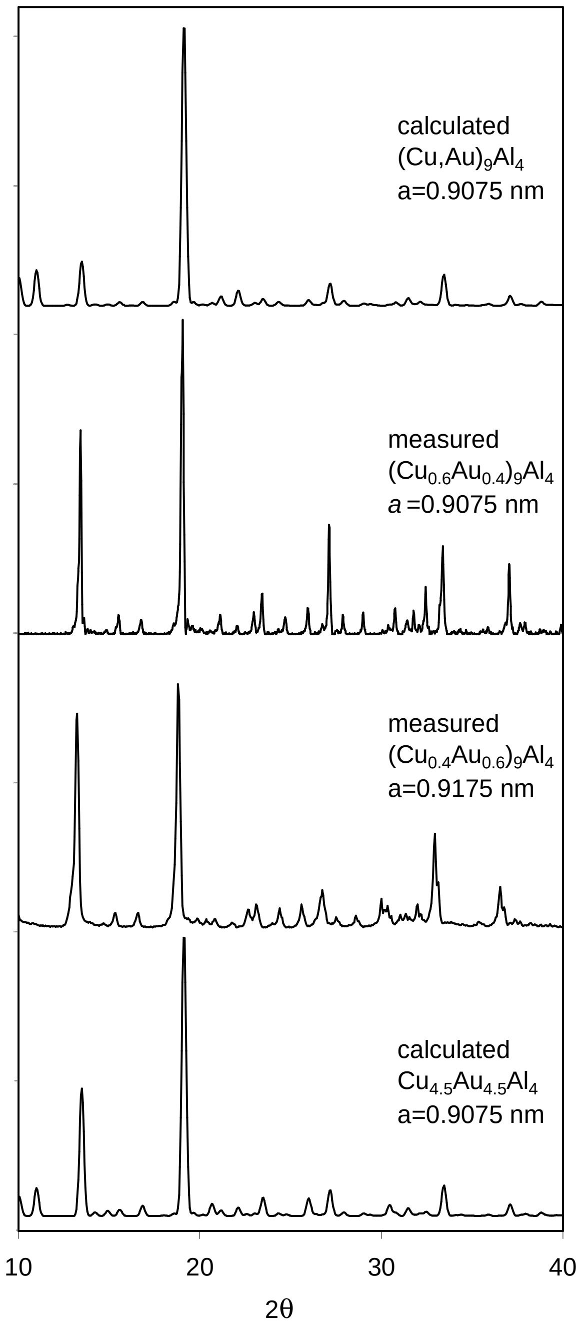

Figure 5. Comparison of calculated and measured spectra for new ternary phase. a. Calculated for Al_4Cu_9 assuming expanded lattice and no ternary ordering of Au and Cu; b. measured for $Al_4(Au_{0.4}Cu_{0.6})_9$; c. measured for $Al_4(Au_{0.6}Cu_{0.4})_9$; d. calculated for $Al_4(Au_{0.6}Cu_{0.4})_9$ assuming ternary ordering.

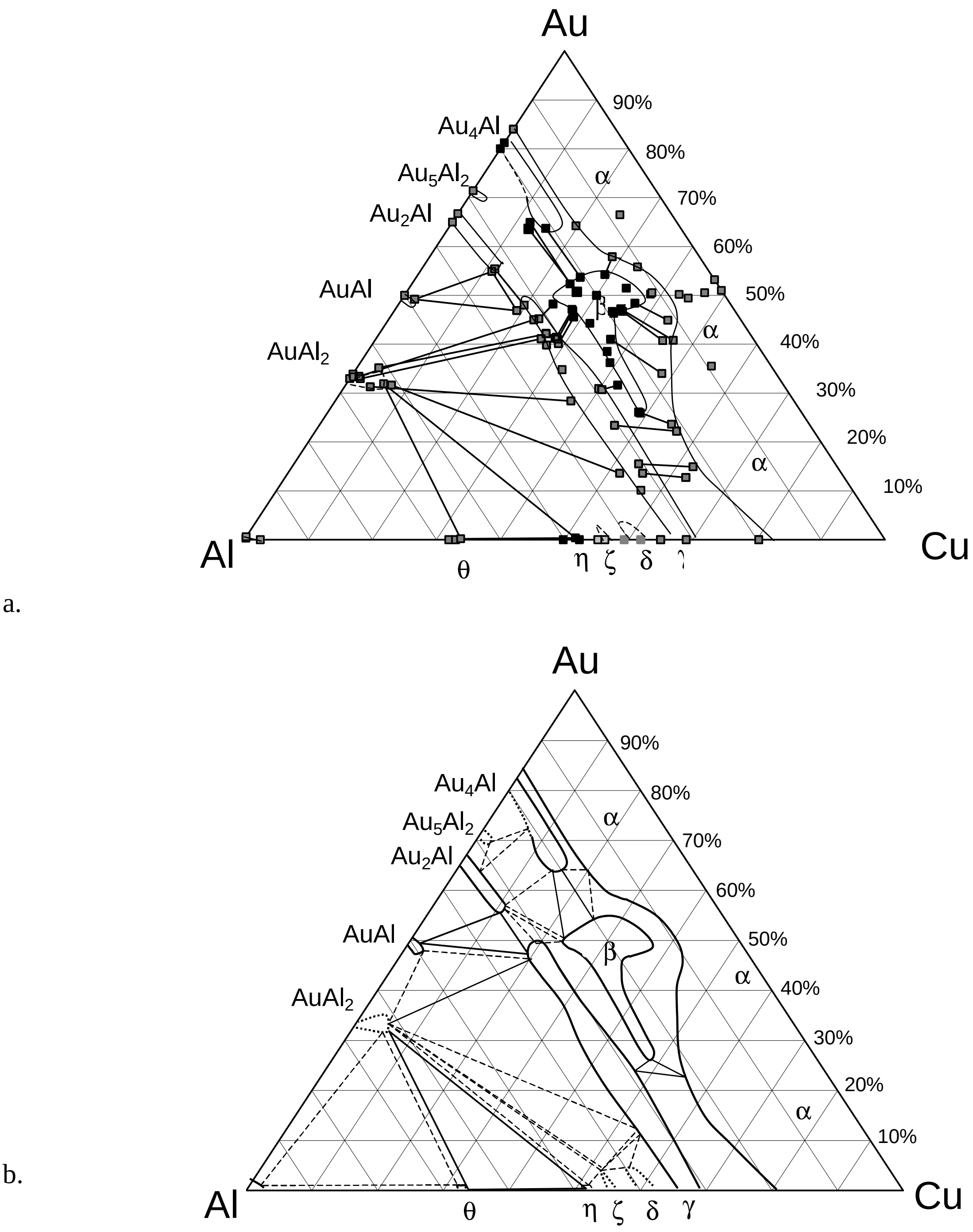

Fig. 6- 500°C section of ternary phase diagram for Al-Au-Cu system. a. data points, tie-lines and postulated phase boundaries; b. postulated phase boundaries and their associated two- and three-phase regions. The position of the 18 carat (75 wt.% Au) line is also shown.

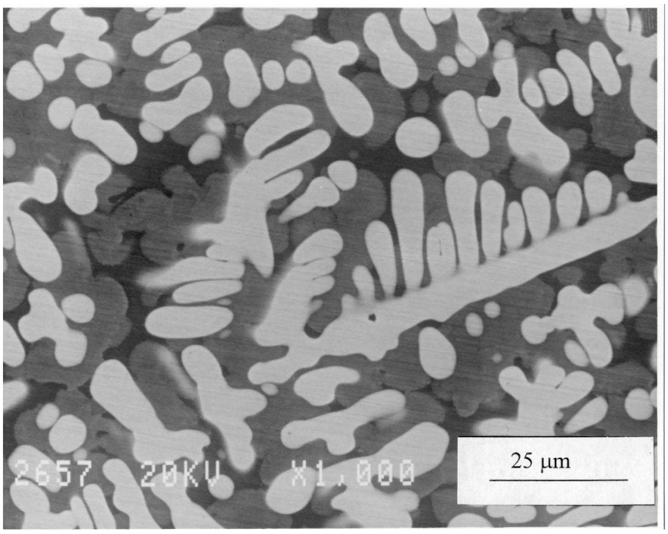

Fig. 7- Microstructure of sample whose overall composition lay within the tie-triangle of Al_2Au-Al_2Cu and AlCu, showing a non-equilibrium microstructure produced by the peritectic consumption of Al_2Au and AlCu to produce Al_2Cu.